Experimental Hematology

Experimental Hematology 2019;78:21–34

REGULAR SUBMISSION

Rats provide a superior model of human stress erythropoiesis

Jingxin Zhang[a,b], Yijie Liu[a], Xu Han[a], Yang Mei[a], Jing Yang[a], Zheng J. Zhang[c], Xinyan Lu[a], and Peng Ji[a]

[a]*Department of Pathology, Feinberg School of Medicine, Northwestern University, Chicago, IL;* [b]*School of Life Science, Zhengzhou University, Zhengzhou, Henan, China;* [c]*Department of Surgery, Feinberg School of Medicine, Northwestern University, Chicago, IL*

(Received 12 July 2019; revised 28 August 2019; accepted 16 September 2019)

Mouse models are widely used to study human erythropoiesis in vivo. One important caveat using mouse models is that mice often develop significant extramedullary erythropoiesis with anemia, which could mask important phenotypes. To overcome this drawback in mice, here we established in vitro and in vivo rat models for the studies of stress erythropoiesis. Using flow cytometry-based assays, we can monitor terminal erythropoiesis in rats during fetal and adult erythropoiesis under steady state and stress conditions. We used this system to test rat erythropoiesis under phenylhydrazine (PHZ)-induced hemolytic stress. In contrast to mice, rats did not have an increased proportion of early-stage erythroid precursors during terminal differentiation in the spleen or bone marrow. This could be explained by the abundant bone marrow spaces in rats that allow sufficient erythroid proliferation under stress. Consistently, the extent of splenomegaly in rats after PHZ treatment was significantly lower than that in mice. The level of BMP4, which was significantly increased in mouse spleen after PHZ treatment, remained unchanged in rat spleen. We further demonstrated that the bone marrow c-Kit positive progenitor population underwent a phenotype shift and became more CD71 positive and erythroid skewed with the expression of maturing erythroid markers under stress in rats and humans. In contrast, the phenotype shift to an erythroid-skewed progenitor population in mice occurred mainly in the spleen. Our study establishes rat in vitro and in vivo erythropoiesis models that are more appropriate and superior for the study of human stress erythropoiesis than mouse models.

Mouse models are the most commonly used laboratory animal models in the study of human erythropoiesis. The identification of several unique cell surface markers on the developing mouse erythroid precursors enables step-by-step cellular and molecular investigations of terminal erythropoiesis from erythroid colony-forming units (CFU-E) to mature red blood cells in vitro. Among these markers, CD71 and Ter119 were first used almost two decades ago to characterize terminal erythropoiesis in mouse bone marrow and spleen [1,2] and later in the fetal liver [3]. About a decade ago, CD44 was introduced to distinguish erythroblasts at different stages of terminal maturation [4]. On the basis of these two systems, several modified versions of flow cytometry-based assays were subsequently developed [5–7].

In vivo studies of erythropoiesis have heavily relied on mice, not only because of the relatively rapid regeneration and short life span of mice, but also because of the ease of obtaining genetically modified animals. A paradigm for these models is the mouse with a homozygous mutation of the β-major globin (Hbb^{th-1} mice) [8].

Offprint requests to: Peng Ji, Department of Pathology, Feinberg School of Medicine, Northwestern University, 303 East Chicago Ave, Ward 3-230, Chicago, IL 60611;
E-mail: ji.peng@northwestern.edu

Supplementary material associated with this article can be found in the online version at https://doi.org/10.1016/j.exphem.2019.09.021.

https://doi.org/10.1016/j.exphem.2019.09.021

Other mouse models with mutations in key erythroid-related genes, such as *EpoR* [9], *Gata1* [10], *Eklf1* [11], *Band-3* [12], *Ankyrin* [13], and *Spectrin* [14], are paramount for our understanding of the transcriptional regulation of erythropoiesis and red cell membrane biology.

Although essential tools for the study of human erythropoiesis, mouse models have their own problems. An important caveat when using mouse models to study human erythropoiesis is that there is significant splenomegaly with anemia in mice. The spleen is an important organ in mice for adult erythropoiesis, especially under stress conditions [15]. Extramedullary erythropoiesis manifested by splenomegaly compensates for anemia, which often masks important phenotypes in mice. This can be revealed in that splenectomy worsens anemia in several anemia mouse models [16]. Nevertheless, stress erythropoiesis mouse models were developed to help understand the pathophysiological responses in vivo [17]. With these tools, research in the past several decades has revealed important pathways in stress erythropoiesis in mice [18,19]. In particular, a spleen-specific bone morphogenetic protein 4 (BMP4)-dependent signaling pathway, which is not present in the bone marrow in mice, drives BFU-E stress erythroid progenitors under various stress conditions [20–23]. However, it is unclear whether the same signaling pathway is also present in humans during stress erythropoiesis.

Rats were used to study erythropoiesis almost a century ago [24]. To a large extent, rats resemble mice in rapid regeneration, short life span, and convenient ex vivo manipulation. Many studies have indicated that rats are more closely related to humans, in whom the spleen plays a far less important role in erythropoiesis under steady state or during stress [24–31]. However, the scarcity of genetically modified rat models prevented their widespread use in mechanistic studies in vivo. In addition, lack of modern technologies, especially flow cytometry-based cell sorting, further limited the characterization and investigation of cellular and molecular mechanisms in rat erythropoiesis compared with that in mouse and human.

In this study, we established rat models for the study of in vitro terminal erythropoiesis and in vivo stress erythropoiesis. When rats, mice, and humans were compared, there was a distinct bone marrow c-Kit–positive progenitor population that underwent a phenotype shift and became more CD71 positive and erythroid skewed by expressing maturing erythroid markers under stress in rats and humans. In contrast, the phenotype shift of c-Kit–positive progenitors to the erythroid-skewed population in mice occurred mainly in the spleen. We conclude that rat models are more suitable for studying human stress erythropoiesis in vivo. Our study provides a valuable resource for the investigation of human stress erythropoiesis using rat models.

Methods

Animal experiments

C57BL/6 mice were purchased from Charles River. ACI rats were purchased from Envigo. Wild-type animals, both males and females, were used. For phenylhydrazine (PHZ, Sigma-Aldrich, St. Louis, MO) treatment, PHZ was dissolved in phosphate-buffered saline (PBS) and injected through the peritoneal route at 40 mg/kg body weight for 3 days. An equal volume of PBS was injected in the control group. Peripheral blood was collected from the mouse or rat tail vein every day, and red blood cells (RBCs) were counted with a Hemavet 950FS (Drew Scientific, FL). Mice and rats were sacrificed for analyses of the bone marrow and spleen when the RBC level recovered halfway to the normal level. To study the stress erythroid progenitors, 100 mg/kg PHZ was injected into rats or mice through the peritoneal route. The animals were sacrificed 36 hours after treatment. The complete blood count was analyzed with the Hemavet 950FS. All animal studies were performed in accordance with the Guidelines for Care and Use of Laboratory Animals and were approved by Institutional Animal Care and Use Committees at Northwestern University.

Flow cytometric assays

For flow cytometric assays in rats, total bone marrow cells were isolated from the hind legs of ACI rats of the ages indicated in the results section. Livers were isolated from E13.5 rat fetuses. The cells were mechanically dissociated by pipetting them in PBS containing 5% fetal bovine serum (Gemini, Sacramento, CA No. 900-108). Single-cell suspensions were prepared by pipetting and passing the tissue through a 40-μm cell strainer (Fisher Scientific, Portsmouth, NH, No. 352340). The following antibodies were used for various stains in the experiments: PE-CD44H (eBioscience, San Diego, CA, No. 12-0444-82), eFlour450-CD45 (eBioscience, No. 48-0461-82), APC-CD71 (eBioscience, No. 17-0710-82), FITC-HIS49 (eBioscience, No. 11-9755-82), PE-c-Kit (Santa Cruz Biotechnology, Dallas, TX, No. sc-19619 PE), Hoechst 33342 (Thermo Fisher, Waltham, MA, No. H3570). Propidium iodide was added to exclude dead cells from analysis. The cells were stained for 20 min at room temperature in the dark and analyzed on an FACS Calibur flow cytometer (BD Biosciences, San Jose, CA). Postacquisition analyses were performed using FlowJo software, version 9.2.3 (Tree Star, Ashland, OR).

For flow cytometric assays in mice, mouse bone marrow, spleen, or fetal liver single-cell suspensions were made as previously mentioned. The following antibodies were used in various experiments: PE-CD71 (eBioscience, No. 12-0711-82), FITC-Ter119 (BioLegend, San Diego, CA, No. 116206), PE-CD44 (eBioscience, No. 12-0441-83), FITC-CD45 (BioLegend, No. 109806), APC-c-Kit (eBioscience, No. 17-1171-82).

For flow cytometric assays in humans, single-cell suspensions were prepared from thawed bone marrow aspirate samples. The following antibodies were used: FITC-c-Kit (eBioscience, No. 11-1178-42), PE-CD235a (eBioscience, No. 12-9987-82), and APC-CD71 (eBioscience, No. 17-0719-42).

Cell culture

Rat bone marrow single-cell suspensions were prepared as described in **Flow Cytometric Assays**. The cells were

labeled with biotin-conjugated lineage-specific antibodies, including HIS49 for erythrocytes (BD Bioscience, No. 550962), HIS48 for granulocytes (eBioscience, No. 13-0570-82), CD45R for B cells (eBioscience, No. 13-0460-82), and CD3 for T cells (BD Biosciences, No. 554831), and incubated on ice for 20 min. The cells were then washed with PBS, suspended with streptavidin particles (BD Biosciences, No. 551728), and incubated on ice for an additional 20 min. Lineage-negative cells were purified using the EasySep column free cell isolation system according to the manufacturer's instructions (Stem Cell Technologies, Cambridge, MA). The purified cells were cultured in Iscove's Modified Dulbecco's Medium (IMDM, Thermo Fisher, No. 12440046) containing 15% fetal bovine serum (Stem Cell Technologies, No. 06200), 1% bovine serum albumin (Stem Cell Technologies, No. 09300), 200 μg/mL holo-transferrin (Sigma-Aldrich, No. T0665), 10 μg/mL recombinant human insulin (Sigma-Aldrich, No. I9278), 2 mmol/L L-glutamine (Hyclone, Marlborough, MA, No. SH30034.01), 10^{-4} mol/L β-mercaptoethanol, and 2 U/mL recombinant human erythropoietin (Amgen, Thousand Oaks, CA). For the culture of fetal liver erythroblasts, total rat fetal liver cells were negatively selected using biotin-conjugated HIS49 (BD Biosciences, No. 550962). The culture medium is the same as that used for rat bone marrow culture. Mouse bone marrow and fetal liver cell cultures were performed as described previously [32–36].

Cytospin and benzidine–Wright–Giemsa stain

Cytospin, benzidine–Wright–Giemsa stains were performed as described previously [7].

Thiazole Orange stain

Rat bone marrow and peripheral blood single-cell suspensions were purified as described in Cell culture. The cells were stained with PE-CD44H (eBioscience, No. 12-0444-82), eFlour450-CD45 (eBioscience, No. 48-0461-82), and 100 ng/mL Thiazole Orange (Sigma-Aldrich, No. 390062) for 20 min in the dark. Propidium iodide was added to exclude dead cells. The cells were analyzed on a FACS Calibur flow cytometer (BD Biosciences). Postacquisition analysis was performed using FlowJo software version 9.2.3 (Tree Star).

BMP4 expression

To analyze BMP4 expression under PHZ-induced acute anemia, mice and rats were injected with 100 mg/kg PHZ through the peritoneal route. The animals were then sacrificed at 0, 12, 24, 36 and 48 hours and day 4. Three animals were included at each time point. Total RNAs were extracted from total bone marrow cells and total spleen cells individually using TRIzol (Ambion, Austin, TX), and cDNA were reverse transcribed from 1 μg of total RNA using qScript cDNA Supermix (Quanta Biosciences, Gaithersburg, MD, No. 95048-100). Quantitative real-time polymerase chain reaction (RT-PCR) was performed using PerfeCTa SYBR Green QPCR FastMix ROX (Quanta Bioscience, No. 95073-012) according to the manufacturer's protocol. The primers used for the QPCR were 18 S forward, GCAATTATTCCCCATGAACG; 18 S reverse, GGCCTCACTAAACCATCCAA; BMP4 forward, TTCCTGGTAACCGAATGCTGA; BMP4 reverse, CCTGAATCTCGGCGACTTTTT. Fluorescence was detected in a QuantStudio 3 System, and cycle threshold values were calculated with the QuantStudio software. BMP4 expression levels were expressed as the difference in *Ct* value (ΔCt) of the target gene and the housekeeping gene (18 S rRNA, eukaryotic 18 S ribosomal RNA) in each sample, and normalized to 18 S rRNA expression.

Human study approval

Bone marrow aspirate samples from posttransplant patients were obtained after receiving informed consent under institutional review board–approved protocols at Northwestern University, Chicago, Illinois.

RNA sequencing

C-kit+ cells were purified from the bone marrow of hind legs of ACI rats 36 hours after peritoneal injection of 100 mg/kg PHZ or an equal volume of PBS, using a Biotin-anti-c-Kit (Abcam, Cambridge, MA, No. ab25022). The total RNA was then isolated using TRIzol (Ambion). The samples were sequenced at BGI (Cambridge, MA) with paired-end 100 bp in the BGISeq-500 platform. Each group had three replicates, and all sequence data were deposited in the Gene Expression Omnibus database (Accession No. GSE122792). Pathway analysis was performed using the DAVID functional annotation bioinformatic tool.

Statistical analysis

Results were analyzed using GraphPad Prism (GraphPad Software, San Diego, CA). All data are expressed as the mean ± SD except where indicated otherwise. All comparisons were carried out using Student *t* test to assess the significance of the results unless otherwise specified. Statistical significance was established at $p < 0.05$.

Results

Development of flow cytometry-based assays for terminal erythropoiesis in rats

To characterize terminal erythropoiesis in rats, we first purified the total bone marrow cells from 3-month-old rats. The cells were stained with CD71 and HIS49, a mouse IgM antibody targeting maturing rat erythroid cells [37], followed by a flow cytometric analysis. We first depleted cell debris and dead cells using forward scatter (FSC) and side scatter (SSC) combined with propidium iodide (PI) (Figure 1A). The gated live rat bone marrow cells were then divided into four populations based on their levels of expression of CD71 and HIS49: Q1 ($CD71^+HIS49^-$); Q2 ($CD71^+HIS49^+$); Q3 ($CD71^-HIS49^+$); and Q4 ($CD71^-HIS49^-$). In parallel, we also stained the cells with Hoechst to reveal the enucleated reticulocytes and mature red blood cells, which indicated that approximately 20% of the cells (Q7) were enucleated in rat bone marrow.

CD44, an erythroid surface glycoprotein that gradually decreases during terminal erythropoiesis, has been

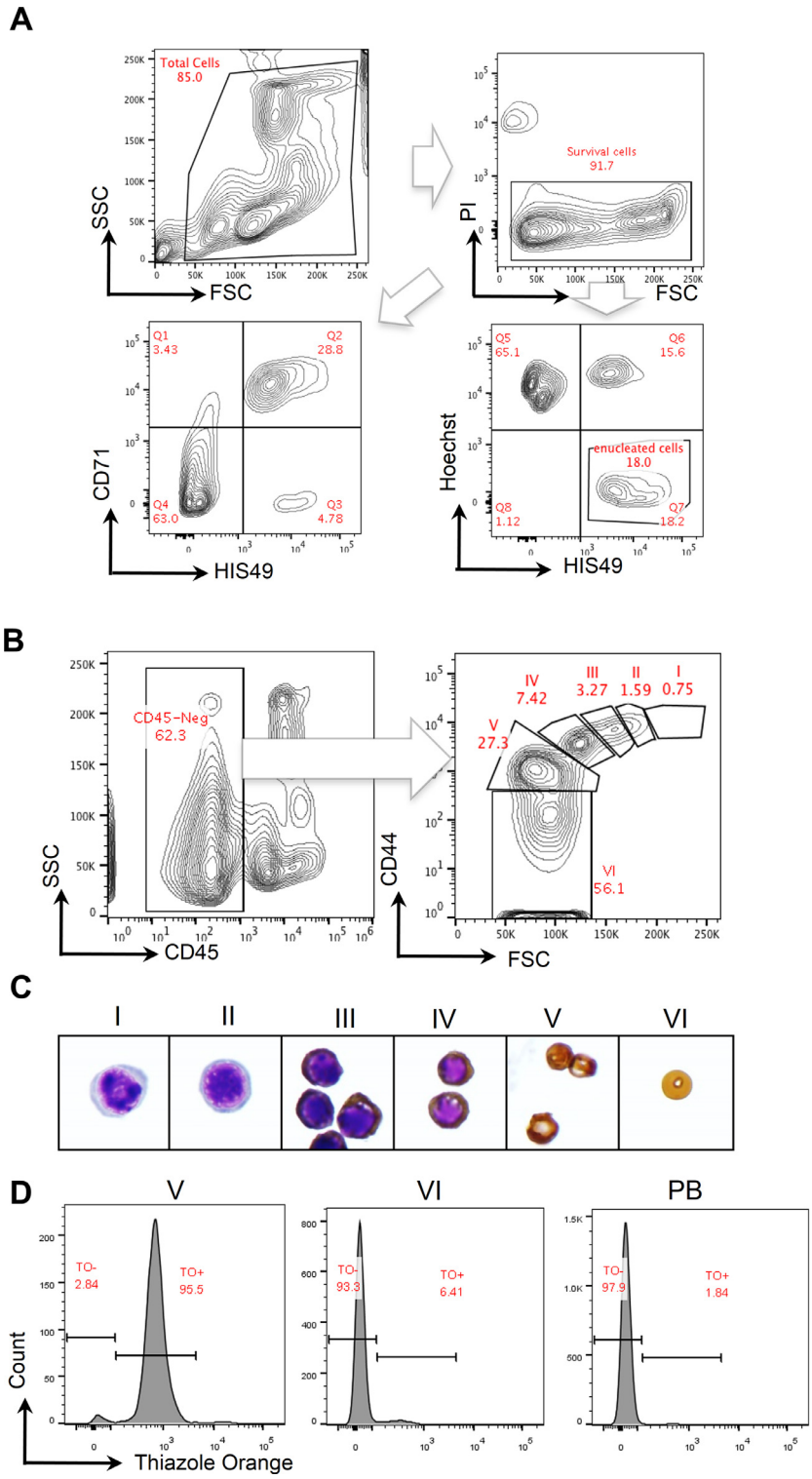

Figure 1. Development of a flow cytometry–based system to characterize rat terminal erythropoiesis in the bone marrow. **(A)** Total bone marrow cells from 3-month-old ACI rats were labeled with anti-CD71, HIS49, and Hoechst. The cells were first gated by forward scatter (FSC), side scatter (SSC), and propidium iodide (PI). The gated live cells were further characterized for their differentiation based on the expression of CD71 and HIS49, and for enucleation based on the percentages of Hoechst-negative and HIS49-positive cells. **(B)** CD45-negative cells gated from live total rat bone marrow cells were separated into six subpopulations (I–VI) based on the level of CD44 and cell size (FSC). **(C)** Populations I–VI from (B) were sorted and stained with benzidine and Wright–Giemsa. Representative images of I–VI are shown and represent the following stages of terminal erythropoiesis: (I) pro-erythroblasts; (II) basophilic erythroblasts; (III) polychromatic erythroblasts; (IV) orthochromatic erythroblasts; (V) reticulocytes; (VI) mature red blood cells. Data are representative of three independent experiments. (**D**) Thiazole orange stain of populations V and VI and peripheral blood (PB) red blood cells.

used in mice to differentiate erythroid precursors at various developmental stages [4]. Using the same strategy, we next stained rat bone marrow cells with antibodies against rat CD45 and CD44, followed by a flow cytometric assay. Gated CD45-negative erythroid cells were further grouped into six distinct populations (I–VI) based on their CD44 expression and cell size (Figure 1B). Benzidine and Giemsa stains of the sorted cells from these populations revealed morphologically recognizable erythroid precursors with cells in populations I to VI representing pro-erythroblasts, basophilic erythroblasts, polychromatic erythroblasts, orthochromatic erythroblasts, reticulocytes, and mature red blood cells, respectively (Figure 1C). Furthermore, we stained populations V and VI with Thiazole Orange to determine the RNA content of these two populations, which indeed revealed significantly high level of RNA in reticulocytes (Figure 1D). Overall, these studies establish a flow cytometry-based system to monitor terminal erythropoiesis in rats.

In vitro culture of rat bone marrow and fetal liver erythroblasts

To study rat terminal erythropoiesis in vitro, we established a culture system to monitor proliferation and differentiation. We used antibodies against markers of differentiated hematopoietic cells in rats to purify lineage-negative bone marrow hematopoietic stem and progenitor cells. The cells were then cultured in erythropoietin-containing medium with transferrin. Over the next 3 days in culture, the cells underwent a significant expansion and reached their highest number at around 72 hours in culture. In comparison, mouse bone marrow lineage-negative cells reached maximum proliferation at around 48 hours in culture (Figure 2A), which is consistent with old studies reporting that mouse bone marrow erythroblasts undergo more rapid cell cycles than rat bone marrow erythroblasts [28,29,38,39]. In comparison to those of rodents, human bone marrow erythroid cells had a greatly extended proliferation time and greater potential for expansion (Figure 2B), possibly because the starting cell type (CD34+ cells) is at an earlier developmental stage than in mice and rats.

To determine the differentiation and enucleation processes of the cultured lineage-negative rat erythroblasts, we performed the same flow cytometric assay as in Figure 1. There was a sharp upregulation of CD71 on day 1 and a gradual gain of HIS49 during culture. The CD71 level decreased slightly on day 3 when most of the cells became HIS49 positive. Enucleated cells appeared on day 2 but reached the maximum on day 3 (Figure 2C). The maximum 20%–30% enucleation rate in cultured rat erythroid cells resembles that of the well-established mouse culture system [7]. As expected, CD44 gradually decreased during culture, forming six populations of different developmental stages on day 3 (Figure 2C), which is also similar to the mouse system.

We next performed the same experiments in rat fetal liver cells. Rat fetal development follows a timeline similar to that of mouse fetal development. On embryonic day 13.5, most of the fetal liver cells in rats were erythroid ($CD71^{+}HIS49^{+}$), with more than 40% of the cells enucleated (Supplementary Figure E1A, online only, available at www.exphem.org). We purified HIS49-negative erythroid precursors and cultured them in erythropoietin-containing medium as the bone marrow culture system. Rat fetal liver erythroid cells proliferated and differentiated more rapidly than their bone marrow counterparts. The cells reached peak proliferation at 48 hours with an approximately 15-fold increase, which is lower than mouse fetal terminal erythroid proliferation (Supplementary Figure E1B). Similar to the bone marrow-derived cells, human fetal-derived cord blood CD34-positive cells had significantly higher proliferative potential compared with the fetal liver cells in mice and rats (Supplementary Figure E1C). We also analyzed the differentiation and enucleation profiles of in vitro cultured rat fetal liver cells. Like mouse fetal liver in vitro culture, rat fetal liver cells underwent gradual upregulation of CD71 and HIS49. Enucleation reached a maximum rate of approximately 20% at 48 hours in culture (Supplementary Figure E1D).

Bone marrow cellularity in rats is distinct from that in mice but similar to that in humans

Bone marrow is the primary organ for erythropoiesis in mammals. One of the important differences between mice and humans in bone marrow histology is that mice are usually hypercellular, whereas human bone marrow contains fat tissues, leaving spaces into which hematopoietic cells expand during stress. We next performed a comprehensive histologic analysis of the bone marrow at various locations in mice and rats. In young mice (2–3 months old), the bone marrow cellularity at most locations (Supplementary Figure E2A–C, online only, available at www.exphem.org), except tail bone (Supplementary Figure E2C), was close to 100%. However, bone marrow cellularity of young rats (3–4 months old, life stage comparable to that of mice) was variable. Among the long bones, the femur and humerus had high bone marrow cellularity (~80%), but tibia and radius contained much fat tissue and had a cellularity close to 50% (Supplementary Figure E2A). The flat bones exhibited high cellularity (~80%) but still contained a considerable amount of fat (Supplementary Figure E2B). Sternum and vertebrae had similar cellularity (~50%–60%). Tail bone was very hypocellular (<5%) (Supplementary Figure E2C). Overall, the bone marrow histology in rats resembles that in humans

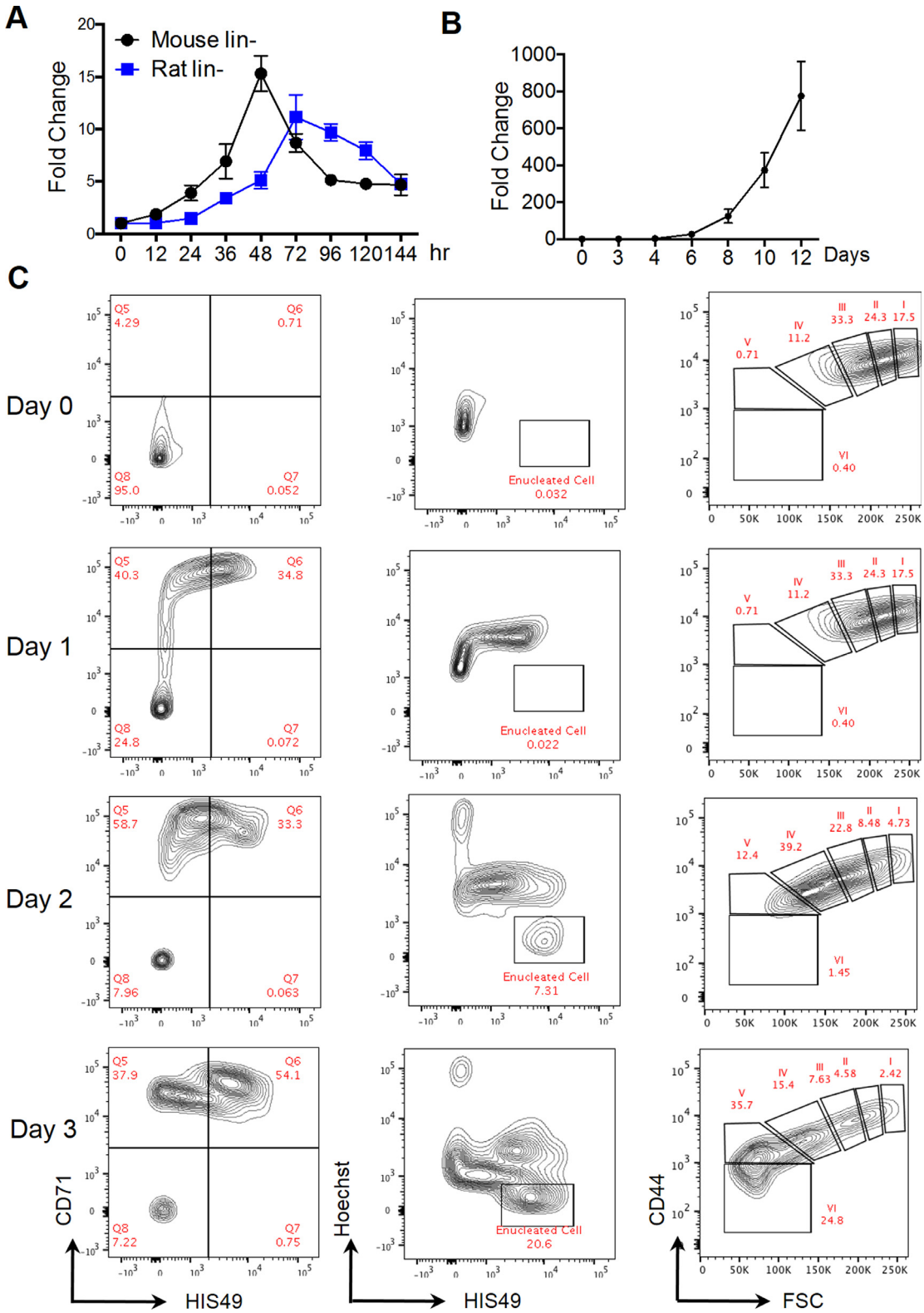

Figure 2. In vitro culture of rat bone marrow lineage-negative cells. **(A)** Bone marrow lineage-negative cells were purified from 6- to 8-week-old wild-type C57BL/6 mice ($n = 3$) and 9- to 12-week-old ACI rats ($n = 3$). One hundred thousand purified cells from rats or mice were cultured in erythropoietin-containing medium for the indicated time. The cells were counted using a hemocytometer at the indicated time. Data are from three independent experiments. **(B)** Human bone marrow CD34-positive cells cultured in erythropoietin-containing medium for the indicated time. The cells were counted using a hemocytometer at the indicated time. **(C)** Cultured rat bone marrow lineage-negative cells from (A) were stained with CD71, HIS49, Hoechst, CD45, and CD44 and analyzed by flow cytometry at the indicated time as in Figure 1.

(Supplementary Figure E2D), which could reflect the similarities in physiology between rats and humans.

Rats and mice are distinct in response to stress erythropoiesis

The culture and flow cytometric assays established in vitro and ex vivo systems in which to study rat terminal erythropoiesis. To investigate rat erythropoiesis in vivo under stress conditions, we injected PHZ peritoneally into rats to induce hemolysis. Mice were treated with the same weight-based dose for comparison. We injected a sublethal dose of PHZ (40 mg/kg) every day for 3 days in rats and mice and monitored their red cell indices daily. Rats and mice have a similar RBC count per equal volume of blood at steady state. After sublethal PHZ treatment, the rats exhibited a decrease in RBCs similar to that in mice. However, rats took a longer time to recover (Figure 3A). The rats also had a more dramatic increase in mean corpuscular volume (MCV) compared with mice (Figure 3A *right*). We sacrificed the animals when they were midway to their full RBC count, which took 5 days for mice and 7 days for rats after their initial PHZ injection. This time point was chosen because the best time to notice differences between rats and mice is when the stress erythroid response is most active. We first examined their spleens given the importance of the spleen in extramedullary erythropoiesis under stress. Compared with mice, rats had significantly less splenomegaly with hemolytic stress (Figure 3B), which may be due to the capability of rat bone marrow to expand in space during stress. Indeed, when we examined bone marrow cellularity after PHZ treatment, mouse bone marrow remained at 100% as in the steady state, whereas rat bone marrow underwent a dramatic increase from ~50% to ~90% (Figure 3C). Because of the lack of space in the bone marrow to expand the erythroid population, mice exhibited a dramatic increase in spleen size with complete replacement of the white pulp by the expanded red pulp. In contrast, although rat spleen enlarged, the architecture remained relatively intact (Figure 3D).

To confirm the morphologic findings, we performed a flow cytometric assay on bone marrow and spleen erythroid cells in mice and rats after PHZ treatment. In mice, the percentages of early-stage erythroid precursors, including pro-erythroblasts, basophilic erythroblasts, and polychromatic erythroblasts, were significantly increased after PHZ treatment in both bone marrow and spleen (Figure 3E, F). In contrast, these early-stage erythroid precursors were not proportionally upregulated in rat bone marrow or spleen after PHZ treatment (Figure 3G, H). These results indicate that mice and rats have distinct responses to hemolytic stress.

Rats and mice have distinct stress-responsive erythroid progenitor populations in bone marrow

Previous studies have reported that mice respond to acute anemia with the expansion of spleen-specific stress erythroid progenitors that require BMP-4 signaling, which is not found in mouse bone marrow [40]. To determine whether rats also have this population under acute anemia stress, we first treated rats and mice with PHZ (100 mg/kg) and determined BMP4 transcription levels in the spleen and bone marrow at different time points. Consistent with a previous report, mouse spleen cells exhibited significantly increased expression of BMP4 transcripts at 36 hours post treatment [40]. In contrast, BMP4 levels remained unchanged in rat spleen after PHZ treatment (Supplementary Figure E3A, online only, available at www.exphem.org). As reported, the increase in BMP4 was not observed in mouse bone marrow post-PHZ treatment. BMP4 levels remained unchanged in rat bone marrow as well (Supplementary Figure E3B). We also observed the same phenotype at later times post-PHZ treatment (data not shown). Taken together, these data suggest that BMP4 signaling may not be required in rats under anemia stress.

As previously reported [40], the stress erythroid progenitor population in mouse spleen was characterized by the transition from c-Kit$^+$CD71$^-$Ter119^{--} (P1) under steady state to c-Kit$^+$CD71$^-$Ter119$^+$ (P3) after hemolytic stress (Figure 4A, D). In contrast with those in mice, c-Kit–positive cells in rat spleen contained mostly CD71$^-$ and HIS49$^-$ cells (P1) under steady state. There was an increase in P2 (c-Kit$^+$CD71^{+-} HIS49$^+$) and P3 (c-Kit$^+$CD71$^-$HIS49$^+$) after PHZ treatment, but the magnitude of change was far less than that in mouse spleen (Figure 4B, D). This is also consistent with the smaller increase in spleen size and partially intact spleen histology after stress in rats (Figure 3B, D). In bone marrow in mice, the major population in c-Kit–positive cells under steady state was CD71 and Ter119 double-negative P1 cells, which remained unchanged during stress as reported (Figure 4E, H) [40]. As for mice, the major population of c-Kit–positive cells in rat bone marrow under steady state was CD71 and HIS49 double-negative P1 cells. However, unlike in mice, there was a dramatic shift to CD71 and HIS49 double-positive P2 cells in rat bone marrow under stress (Figure 4F, H). The c-Kit–positive population indeed increased proportionally in bone marrow and spleen in both mice and rats (Figure 4C, G). Overall, these results indicate that rat bone marrow is the major organ for stress erythropoiesis. These c-Kit$^+$/erythroid-skewed stress erythroid progenitors, mostly cells in the P2 population in Figure 4, are primarily in the bone marrow in rats, whereas this stress erythroid progenitor population is mainly in the spleen in mice.

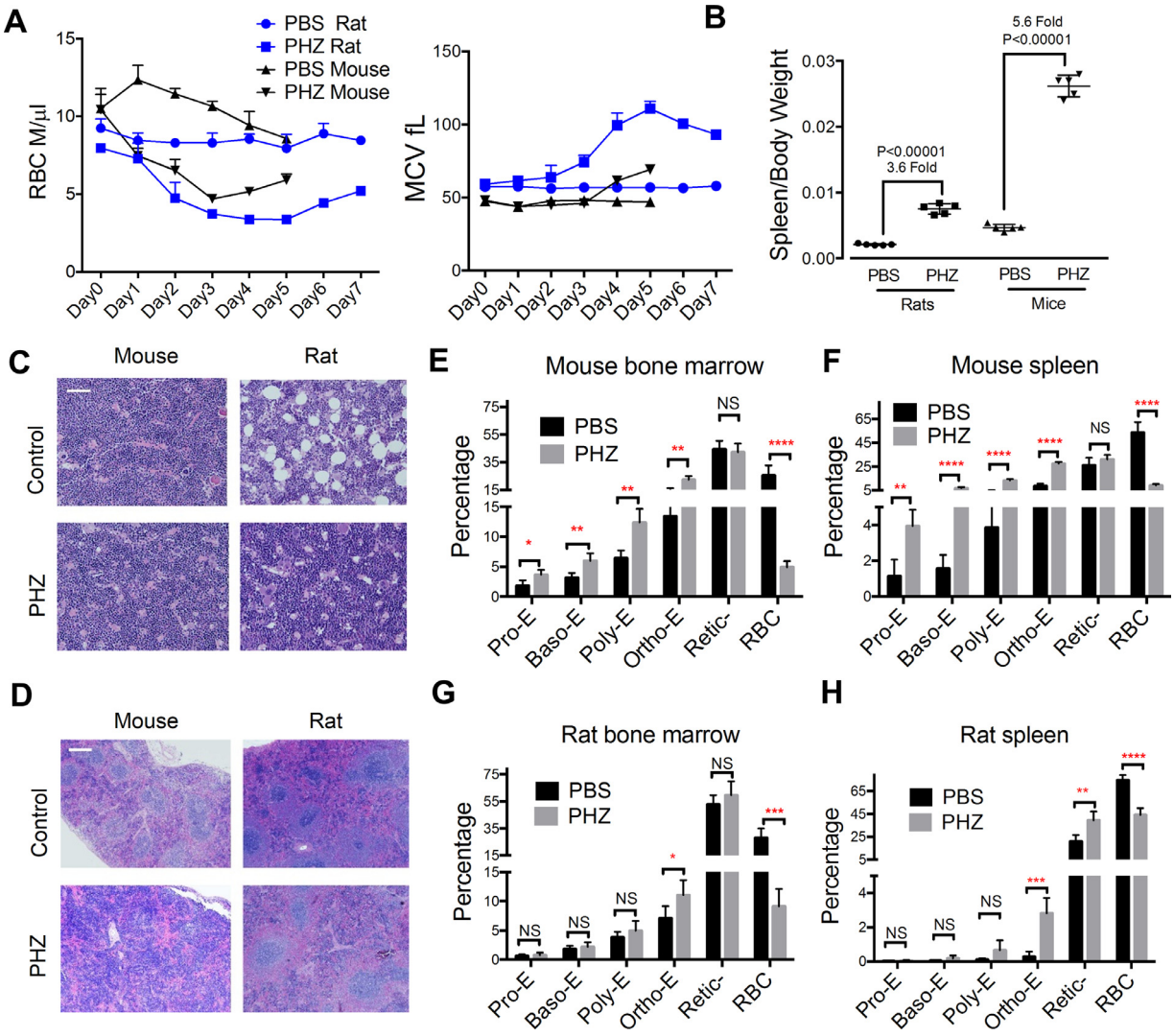

Figure 3. Rats and mice are distinct during stress erythropoiesis. **(A)** Three- to four-month-old wild-type ACI rats and 2- to 3-month-old wild-type C57BL/6 mice were injected with PHZ peritoneally at 40 mg/kg daily for 3 days. Peripheral blood was collected for analyses of RBC count and MCV daily at the indicated time. The animals were sacrificed for histologic and flow cytometry assays when the RBC levels had recovered to half of the normal level (day 5 for mice and day 7 for rats). $n = 5$ in each group. (B) The spleens of the sacrificed animals in (A) were harvested and their weight relative to body weight was measured. **(C, D)** Histologic examination of (C) bone marrow and (D) spleen from animals sacrificed in (A). Bars = 100 μm. **(E, F)** Flow cytometric analyses of different stages of terminal erythroblasts based on CD44 and FSC as in Figure 1 in the bone marrow and spleen of mice sacrificed in (A). Data are expressed as the mean ± SD. *p < 0.05, **p < 0.01, ***p < 0.001. *NS*=Nonsignificant. **(G, H)** Same as for (E) and (F) except rat bone marrow and spleen cells were analyzed.

More importantly, we analyzed stress erythroid progenitors in adult human patients within 30 days of bone marrow transplantation for hematologic malignancies. The transplanted donor erythroid progenitors are known to undergo active proliferation in response to the transplantation stress [41]. We analyzed the c-Kit −positive cells of the frozen bone marrow aspirate from bone marrow transplant patients and compared the results with those of samples from normal adult bone marrow. Under the normal steady-state situation, the main subpopulation in c-Kit−positive cells was CD71 and CD235a (glycophorin A) double-negative cells (P1) and $CD71^{+}CD235a^{-}$(P2) subpopulations, which is similar to the composition of c-Kit−positive cells in rat bone marrow (Figure 5A). Under bone marrow transplantation stress, cell composition shifted, with a significant increase in P2 and decrease in P1 (Figure 5B, C), similar to rat bone marrow during stress erythropoiesis.

Transcriptomic profile of c-Kit+ cells in rat bone marrow under stress

We next performed an RNA-sequencing analysis of the c-Kit−positive cells under stress to identify novel

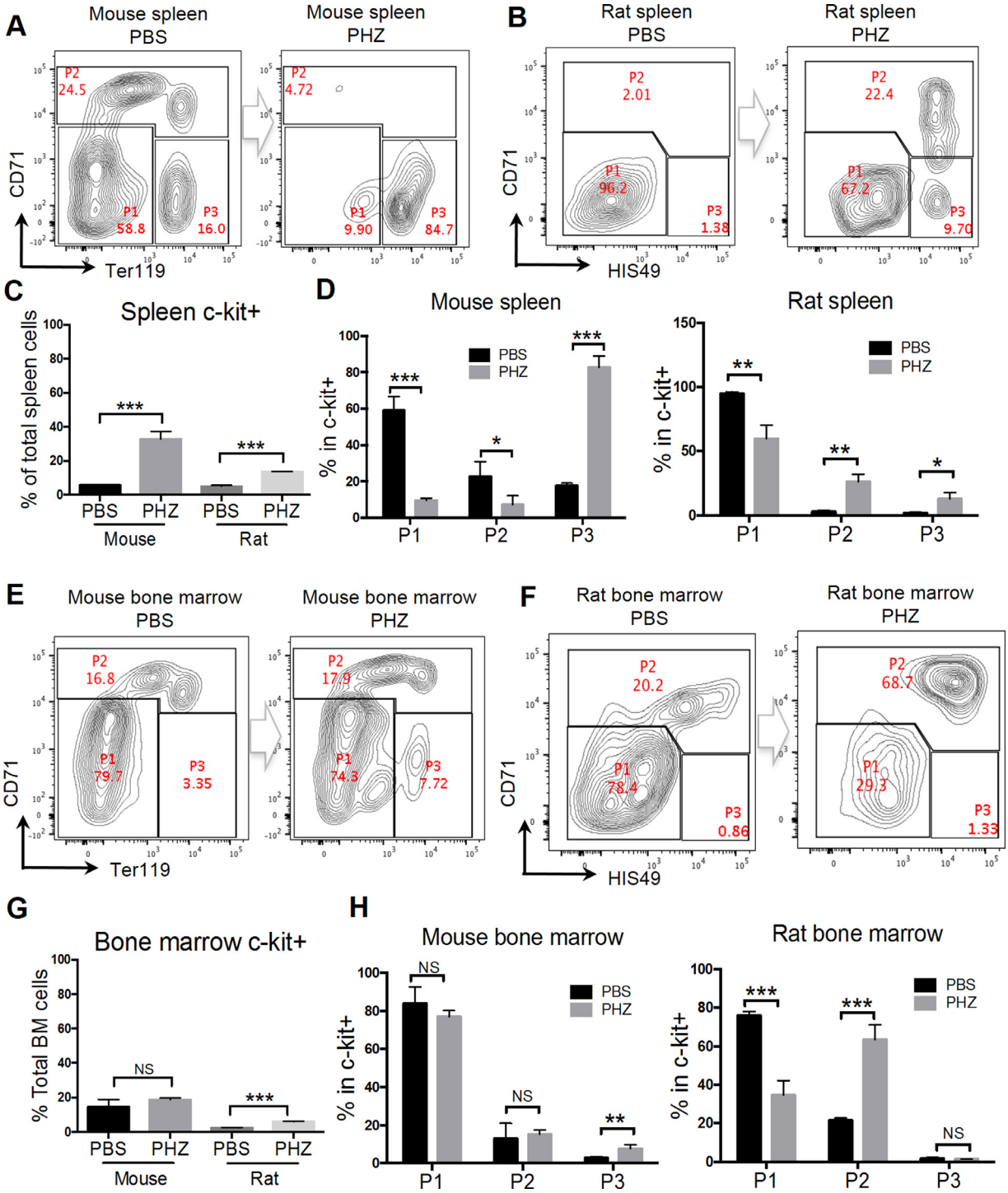

Figure 4. Rat bone marrow is the major organ for stress erythropoiesis. Three-month-old wild-type ACI rats ($n = 9$) and 2-month-old wild-type C57BL/6 mice ($n = 9$) were injected with 100 mg/kg PHZ and sacrificed 36 hours after treatment. **(A, B)** Flow cytometric analyses of mouse (A) and rat (B) spleen c-Kit−positive cells with the indicated markers under PHZ or PBS treatment. **(C, D)** Quantitative analyses of c-Kit−positive cells **(C)** and percentages of P1 ($CD71^{-}Ter119/HIS49^{-}$), P2 ($CD71^{+}Ter119/HIS49^{med}$), and P3 ($CD71^{-}Ter119/HIS49^{+}$) subpopulations in c-Kit −positive cells. **(E, F)** Same as in (A) and (B) except bone marrow cells were analyzed. **(G, H)** Same as in (C) and (D) except bone marrow cells were analyzed. *$p < 0.05$, **$p < 0.01$, ***$p < 0.001$. The data are representative of three independent experiments. *BM*=Bone marrow; *NS*=nonsignificant.

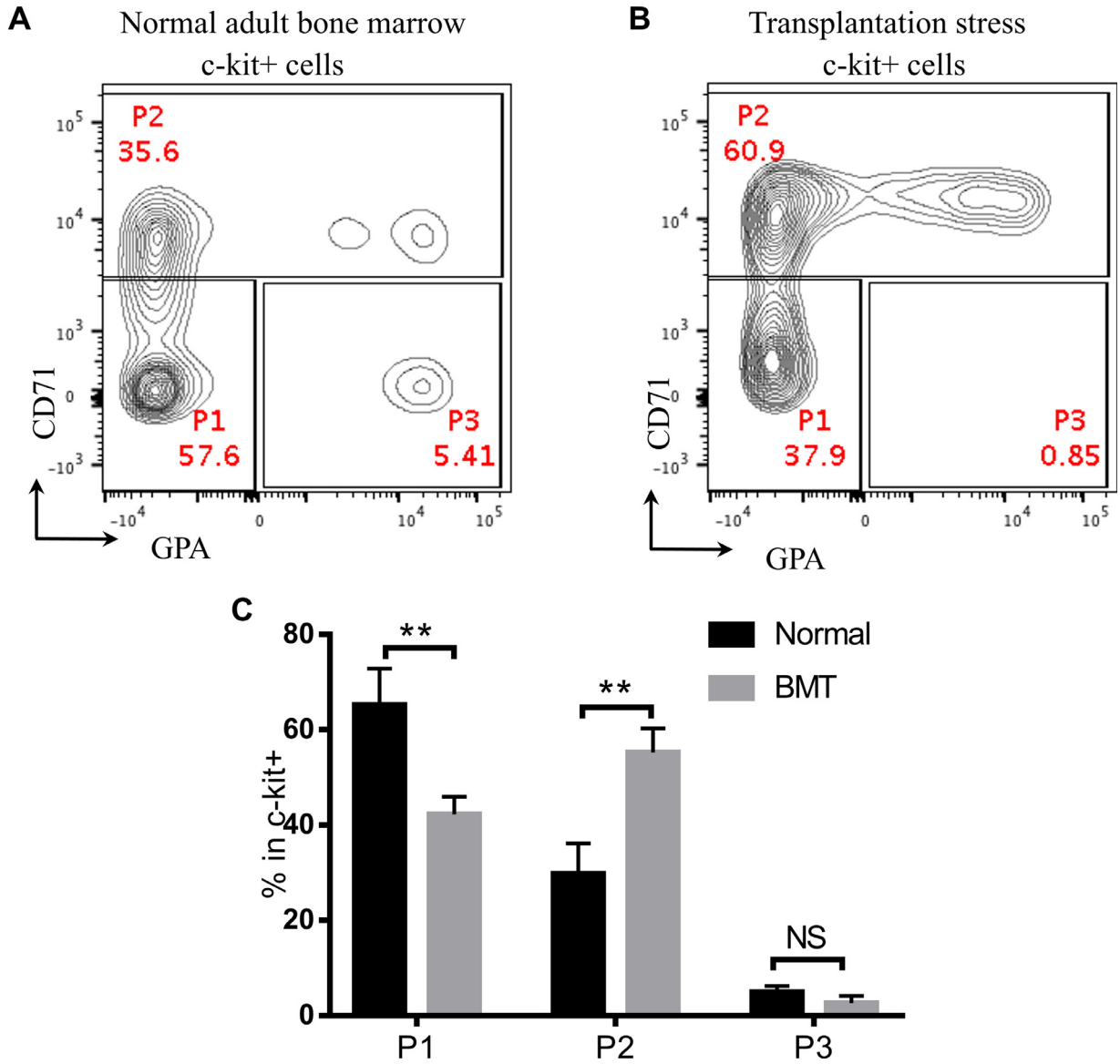

Figure 5. Increase in c-Kit$^+$/erythroid-skewed population in human bone marrow during stress erythropoiesis. **(A)** Flow cytometric analysis of bone marrow aspirates obtained from normal (lymphoma staging−negative) and bone marrow−transplanted patients. C-Kit−positive cells were gated for the analysis of CD71 and CD235a expression levels. **(B)** Quantitative analysis of different subpopulations of c-Kit−positive cells in (A). $N = 4$ in each group. $^{**}p < 0.01$. *BMT*=bone marrow transplantation; *NS*=nonsignificant.

factors and pathways involved in rat stress erythropoiesis. Pairwise comparisons between PBS- and PHZ-treated c-Kit−positive cells in rat bone marrow revealed high Pearson correlation coefficients among replicates (range: 0.96−0.99). The differentially expressed genes were analyzed and illustrated in a volcanic map (Figure 6A). The upregulated genes include those important for cell cycling, metabolism, DNA replication and RNA transport. The downregulated genes are involved in several immune-related pathways (Figure 6B). Among these genes, Fgf23 and GPBP1L1 are highly upregulated in c-Kit−positive cells from PHZ-treated rats (Figure 6C). These highly upregulated genes could be potentially significant in bone marrow responses to stress erythropoiesis in rats; further research is required.

Discussion

Our study establishes rat in vitro erythroid cell culture and in vivo stress erythropoiesis models through which we can monitor the differentiation, proliferation, and enucleation of rat erythroid cells step by step in different hematopoietic organs. When comparing mouse and rat cultured erythroid cells, several similarities were observed during steady-state erythropoiesis. Bone marrow and fetal liver erythroid differentiation in rodents exhibited rapid kinetics compared with that in humans.

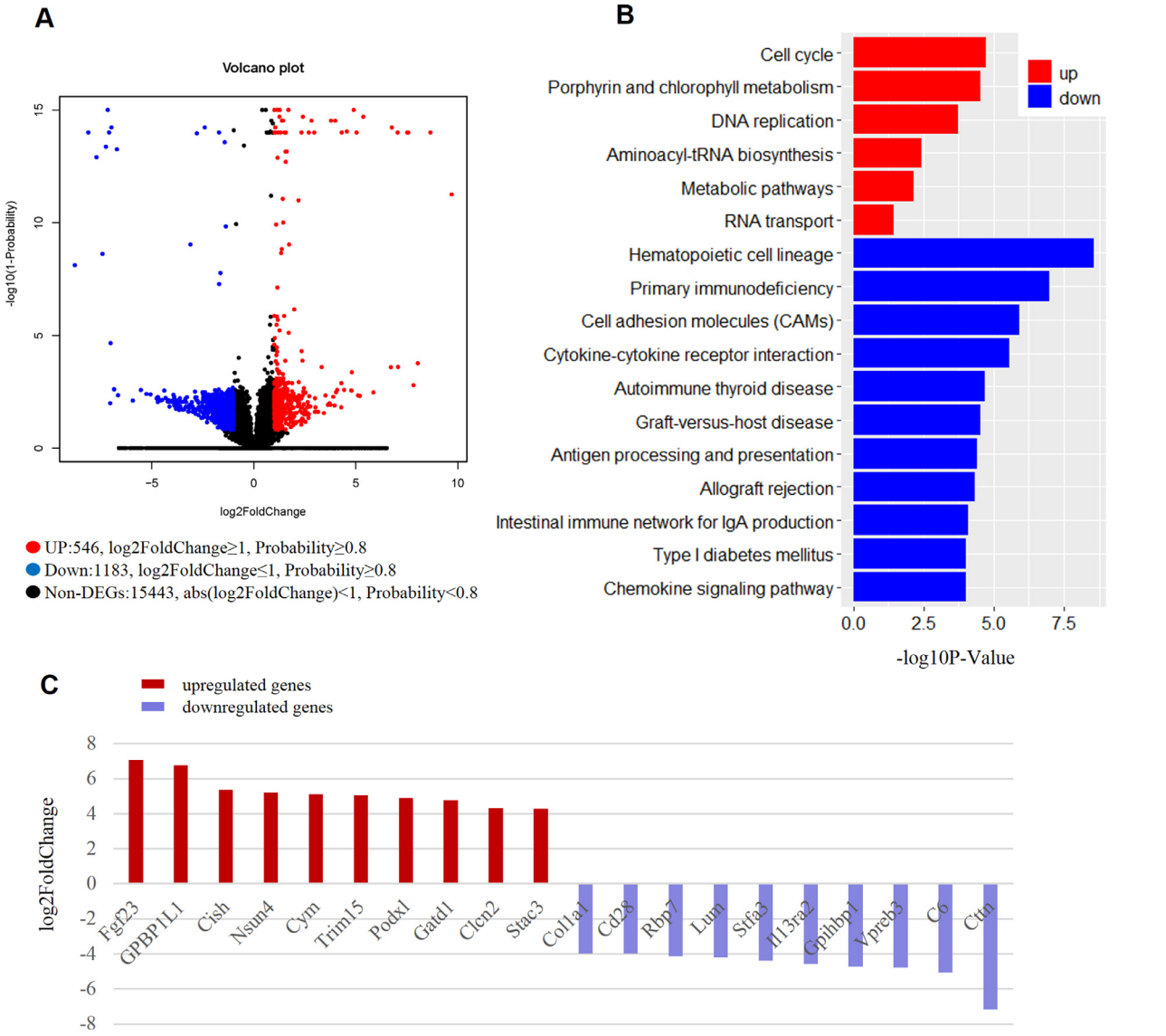

Figure 6. Transcriptome analysis of c-kit+ cells from rats under stress erythropoiesis. ACI rats were injected with PHZ at 100 mg/kg or PBS and sacrificed 36 hours after injection. Bone marrow c-Kit+ cells from these mice were purified for RNA-sequencing analyses. Each group contains three samples. **(A)** Volcano plot of differentially expressed genes. The *x* axis represents $\log_2$-transformed fold change. The *y* axis represents −log transformed significance. *Red* and *blue* points represent up- and downregulated differentially expressed genes, respectively. Gray points represent nondifferentially expressed genes. **(B)** Pathway functional enrichment of differentially expressed genes. Top upregulated (*red*) and downregulated (*blue*) pathways are listed. **(C)** Top 10 upregulated (*red*) and top 10 downregulated (*blue*) genes in c-Kit+ cells from ACI rat bone marrow after PHZ injection.

The enucleation rate in culture was also lower in both rats and mice when compared with that in humans. These differences between rodents and humans can be intrinsic but could also be related to the distinctions in the differentiation stages of the starting cell types in culture.

The differences in erythropoiesis between rats and mice are also significant, specifically those for stress erythropoiesis. Three major differences in stress erythropoiesis were noted between rats and mice of comparable age. Importantly, the features seen in rats are shared by humans under stress erythropoiesis: (1) The low bone marrow cellularity in rats provides expandable spaces for the proliferation of erythroid cells during stress. (2) Under stress conditions, extramedullary erythropoiesis plays a less important role in rats. (3) More importantly, the bone marrow c-Kit−positive stress progenitor population undergoes a phenotype shift and becomes more CD71 positive and erythroid-skewed under stress in rats and humans. In contrast, the phenotype shift to the erythroid-skewed stress progenitor population in mice occurs mainly in the spleen (Figure 7).

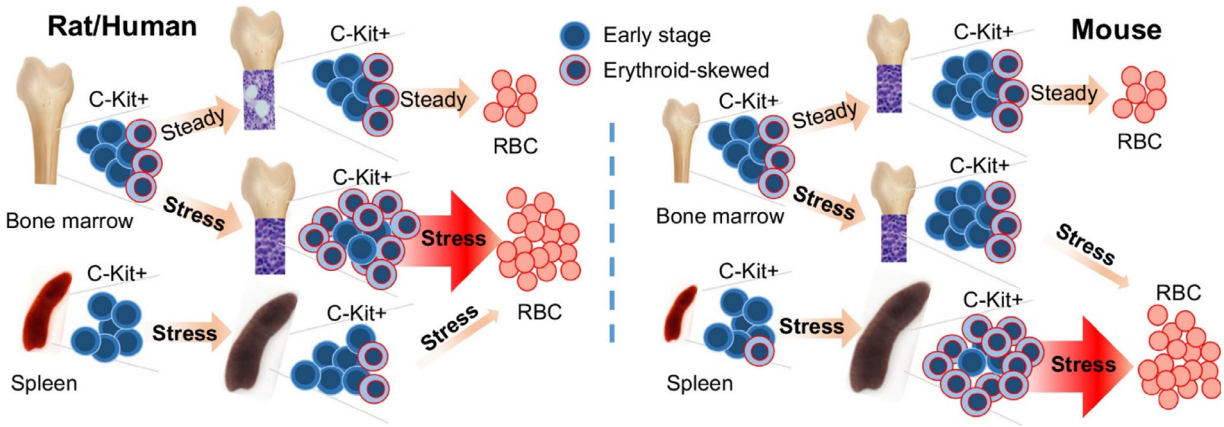

Figure 7. Schematics of the c-Kit–positive erythroid progenitor populations during steady state and stress erythropoiesis in rat, human, and mouse. Rat and human (*left*) use primarily the bone marrow for stress erythropoiesis, whereas mouse (*right*) uses the spleen.

We propose that the similarities between rats and humans during stress erythropoiesis are due mainly to the expandable bone marrow spaces in both species (Figure 3). This is supported by the PHZ treatment experiments in rats (Figure 3C) and well-documented bone marrow hypercellularity with erythroid hyperplasia in humans during hemolytic anemia [42]. Furthermore, studies performed more than two decades ago using a splenectomy approach indicated that splenic erythropoiesis was negligible for the recovery from anemia in rats [43]. In contrast, splenectomy in mice in an infection-induced anemia model resulted in worsened anemia after the surgery [16], which is consistent with the critical role of the spleen in stress erythropoiesis in mice. Indeed, a unique BMP4-dependent stress erythroid progenitor population in mouse spleen that undergoes a transition from c-Kit^{+}CD71^{-}Ter119^{-}(P1) to c-Kit^{+}CD71^{-}Ter119^{+} (P3) under stress conditions has been reported [40]. However, this population was not identified in rat spleen in our study. In contrast, the phenotype shift in the c-Kit–positive stress erythroid progenitor population in rats, from CD71 and HIS49 double negative to double positive, occurs mainly in the bone marrow (Figures 4 and 7).

The properties of stress response in rats closely mimic those in humans. Our analyses of patients who have undergone bone marrow transplantation revealed that the c-Kit–positive progenitor population exhibited a significant increase in CD71 levels. Consistent with our findings, a previous report revealed that CD34-positive cells in patients with sickle cell anemia exhibit strong upregulation of CD71 and CD235a [44]. In addition, it was observed that splenectomy before allogeneic hematopoietic stem cell transplantation in patients with myelofibrosis was associated with improved overall survival and event-free survival [45], indicating a negligible role of the spleen during stress hematopoiesis. Together the information strongly supports the bone marrow as the major organ for stress erythropoiesis in humans.

Our study indicates that rat models are more appropriate and superior for the study of human stress erythropoiesis than mouse models. Given the similarities between rats and humans in the response to anemia, novel pathways or genes involved in stress erythropoiesis could be shared by these two species. Our gene expression profiling study revealed genes that are upregulated in stress erythropoiesis in rat bone marrow. Future functional studies will provide important information regarding the mechanisms underlying this gene upregulation during stress erythropoiesis. Technological advances in the CRISPR-Cas9–mediated genome editing system would also make it easy to generate genetically modified rat models for in vivo studies of these genes in rat during stress erythropoiesis.

Acknowledgments

This work was supported in part by National Institute of Diabetes and Digestive and Kidney Disease (NIDDK) Grant DK102718 (PJ), Department of Defense Grant CA140119 (PJ), and a Leukemia and Lymphoma Society Scholar Award to PJ.

We thank the flow cytometry core facility at the Feinberg School of Medicine for the help with flow cytometric analyses.

Conflict of interest disclosure

The authors declare no competing financial interests related to this work.

References

1. Kina T, Ikuta K, Takayama E, et al. The monoclonal antibody TER-119 recognizes a molecule associated with glycophorin A and specifically marks the late stages of murine erythroid lineage. Br J Haematol. 2000;109:280–287.

2. Socolovsky M, Nam H, Fleming MD, et al. Ineffective erythropoiesis in Stat5a(−/−)5b(−/−) mice due to decreased survival of early erythroblasts. Blood. 2001;98:3261–3273.
3. Zhang J, Socolovsky M, Gross AW, et al. Role of Ras signaling in erythroid differentiation of mouse fetal liver cells: functional analysis by a flow cytometry-based novel culture system. Blood. 2003;102:3938–3946.
4. Chen K, Liu J, Heck S, et al. Resolving the distinct stages in erythroid differentiation based on dynamic changes in membrane protein expression during erythropoiesis. Proc Natl Acad Sci USA. 2009;106:17413–17418.
5. Liu J, Zhang J, Ginzburg Y, et al. Quantitative analysis of murine terminal erythroid differentiation in vivo: novel method to study normal and disordered erythropoiesis. Blood. 2013;121:e43–e49.
6. Hu J, Liu J, Xue F, et al. Isolation and functional characterization of human erythroblasts at distinct stages: implications for understanding of normal and disordered erythropoiesis in vivo. Blood. 2013;121:3246–3253.
7. Ji P, Jayapal SR, Lodish HF. Enucleation of cultured mouse fetal erythroblasts requires Rac GTPases and mDia2. Nat Cell Biol. 2008;10:314–321.
8. Skow LC, Burkhart BA, Johnson FM, et al. A mouse model for beta-thalassemia. Cell. 1983;34:1043–1052.
9. Wu H, Liu X, Jaenisch R, et al. Generation of committed erythroid BFU-E and CFU-E progenitors does not require erythropoietin or the erythropoietin receptor. Cell. 1995;83:59–67.
10. Gutierrez L, Tsukamoto S, Suzuki M, et al. Ablation of Gata1 in adult mice results in aplastic crisis, revealing its essential role in steady-state and stress erythropoiesis. Blood. 2008;111:4375–4385.
11. Nuez B, Michalovich D, Bygrave A, et al. Defective haematopoiesis in fetal liver resulting from inactivation of the EKLF gene. Nature. 1995;375:316–318.
12. Peters LL, Shivdasani RA, Liu SC, et al. Anion exchanger 1 (band 3) is required to prevent erythrocyte membrane surface loss but not to form the membrane skeleton. Cell. 1996;86:917–927.
13. White RA, Birkenmeier CS, Lux SE, et al. Ankyrin and the hemolytic anemia mutation, nb, map to mouse chromosome 8: presence of the nb allele is associated with a truncated erythrocyte ankyrin. Proc Natl Acad Sci USA. 1990;87:3117–3121.
14. Kaysser TM, Wandersee NJ, Bronson RT, et al. Thrombosis and secondary hemochromatosis play major roles in the pathogenesis of jaundiced and spherocytic mice, murine models for hereditary spherocytosis. Blood. 1997;90:4610–4619.
15. Chen D, Kaul DK. Rheologic and hemodynamic characteristics of red cells of mouse, rat and human. Biorheology. 1994;31:103–113.
16. Anosa V, Jennings FW, Urquhart GM. The effect of splenectomy on anaemia in *Trypanosoma brucei* infection of mice. J Comp Pathol. 1977;87:569–579.
17. Schubert TE, Obermaier F, Ugocsai P, et al. Murine models of anaemia of inflammation: extramedullary haematopoiesis represents a species specific difference to human anaemia of inflammation that can be eliminated by splenectomy. Int J Immunopathol Pharmacol. 2008;21:577–584.
18. Paulson RF, Shi L, Wu DC. Stress erythropoiesis: new signals and new stress progenitor cells. Curr Opin Hematol. 2011;18:139–145.
19. Bennett LF, Liao C, Paulson RF. Stress erythropoiesis model systems. Methods Mol Biol. 2018;1698:91–102.
20. Lenox LE, Perry JM, Paulson RF. BMP4 and Madh5 regulate the erythroid response to acute anemia. Blood. 2005;105:2741–2748.
21. Perry JM, Harandi OF, Paulson RF. BMP4, SCF, and hypoxia cooperatively regulate the expansion of murine stress erythroid progenitors. Blood. 2007;109:4494–4502.
22. Porayette P, Paulson RF. BMP4/Smad5 dependent stress erythropoiesis is required for the expansion of erythroid progenitors during fetal development. Dev Biol. 2008;317:24–35.
23. Perry JM, Harandi OF, Porayette P, et al. Maintenance of the BMP4-dependent stress erythropoiesis pathway in the murine spleen requires hedgehog signaling. Blood. 2009;113:911–918.
24. Hammett FS, Nowrey JE. The erythropoietic action of germanium dioxide: II. The source of the erythrocythemia produced by germanium dioxide in the albino rat. J Exp Med. 1922;35:507–513.
25. Baxter CF, Belcher EH, Harriss EB, et al. Anaemia and erythropoiesis in the irradiated rat: an experimental study with particular reference to techniques involving radioactive iron. Br J Haematol. 1955;1:86–103.
26. Stohlman F Jr, Brecher G. Stimulation of erythropoiesis in sublethally irradiated rats by a plasma factor. Proc Soc Exp Biol Med. 1956;91:1–4.
27. Garcia JF. Changes in blood, plasma and red cell volume in the male rat, as a function of age. Am J Physiol. 1957;190:19–24.
28. Hulse EV. Recovery of erythropoiesis after irradiation: a quantitative study in the rat. Br J Haematol. 1963;9:365–375.
29. Tarbutt RG. A study of erythropoiesis in the rat. Exp Cell Res. 1967;48:473–483.
30. Vacek A, Bartonickova A, Tkadlecek L. Age dependence of the number of the stem cells in haemopoietic tissues of rats. Cell Tissue Kinet. 1976;9:1–8.
31. Mohandas N, Prenant M. Three-dimensional model of bone marrow. Blood. 1978;51:633–643.
32. Zhao B, Yang J, Ji P. Chromatin condensation during terminal erythropoiesis. Nucleus. 2016;7:425–429.
33. Zhao B, Mei Y, Yang J, et al. Erythropoietin-regulated oxidative stress negatively affects enucleation during terminal erythropoiesis. Exp Hematol. 2016;44:975–981.
34. Zhao B, Mei Y, Schipma MJ, et al. Nuclear condensation during mouse erythropoiesis requires caspase-3-mediated nuclear opening. Dev Cell. 2016;36:498–510.
35. Mei Y, Zhao B, Yang J, et al. Ineffective erythropoiesis caused by binucleated late-stage erythroblasts in mDia2 hematopoietic specific knockout mice. Haematologica. 2016;101:e1–e5.
36. Zhao B, Mei Y, Cao L, et al. Loss of pleckstrin-2 reverts lethality and vascular occlusions in JAK2V617F-positive myeloproliferative neoplasms. J Clin Invest. 2018;128:125–140.
37. Hermans MH, Opstelten D. In situ visualization of hemopoietic cell subsets and stromal elements in rat and mouse bone marrow by immunostaining of frozen sections. J Histochem Cytochem. 1991;39:1627–1634.
38. Monette FC, LoBue J, Gordon AS, et al. Erythropoiesis in the rat: differential rates of DNA synthesis and cell proliferation. Science. 1968;162:1132–1134.
39. Pantel K, Loeffler M, Bungart B, et al. A mathematical model of erythropoiesis in mice and rats: Part 4. Differences between bone marrow and spleen. Cell Tissue Kinet. 1990;23:283–297.
40. Harandi OF, Hedge S, Wu DC, et al. Murine erythroid short-term radioprotection requires a BMP4-dependent, self-renewing population of stress erythroid progenitors. J Clin Invest. 2010;120:4507–4519.
41. Davies SV, Cavill I, Bentley N, et al. Evaluation of erythropoiesis after bone marrow transplantation: quantitative reticulocyte counting. Br J Haematol. 1992;81:12–17.
42. Tabbara IA. Hemolytic anemias. Diagnosis and management. Med Clin North Am. 1992;76:649–668.

43. Hirofumi Nagai FC, Satoshi Sasaki, Hiroaki Miyajima. Negligible contribution of splenic erythropoiesis to recovery from anemia in rats. J Toxicol Pathol. 1993;6:241–249.
44. Luck L, Zeng L, Hiti AL, et al. Human CD34(+) and CD34(+) CD38(−) hematopoietic progenitors in sickle cell disease differ phenotypically and functionally from normal and suggest distinct subpopulations that generate F cells. Exp Hematol. 2004;32:483–493.
45. Robin M, Zine M, Chevret S, et al. The impact of splenectomy in myelofibrosis patients before allogeneic hematopoietic stem cell transplantation. Biol Blood Marrow Transplant. 2017;23:958–964.

Appendix. Supplementary materials

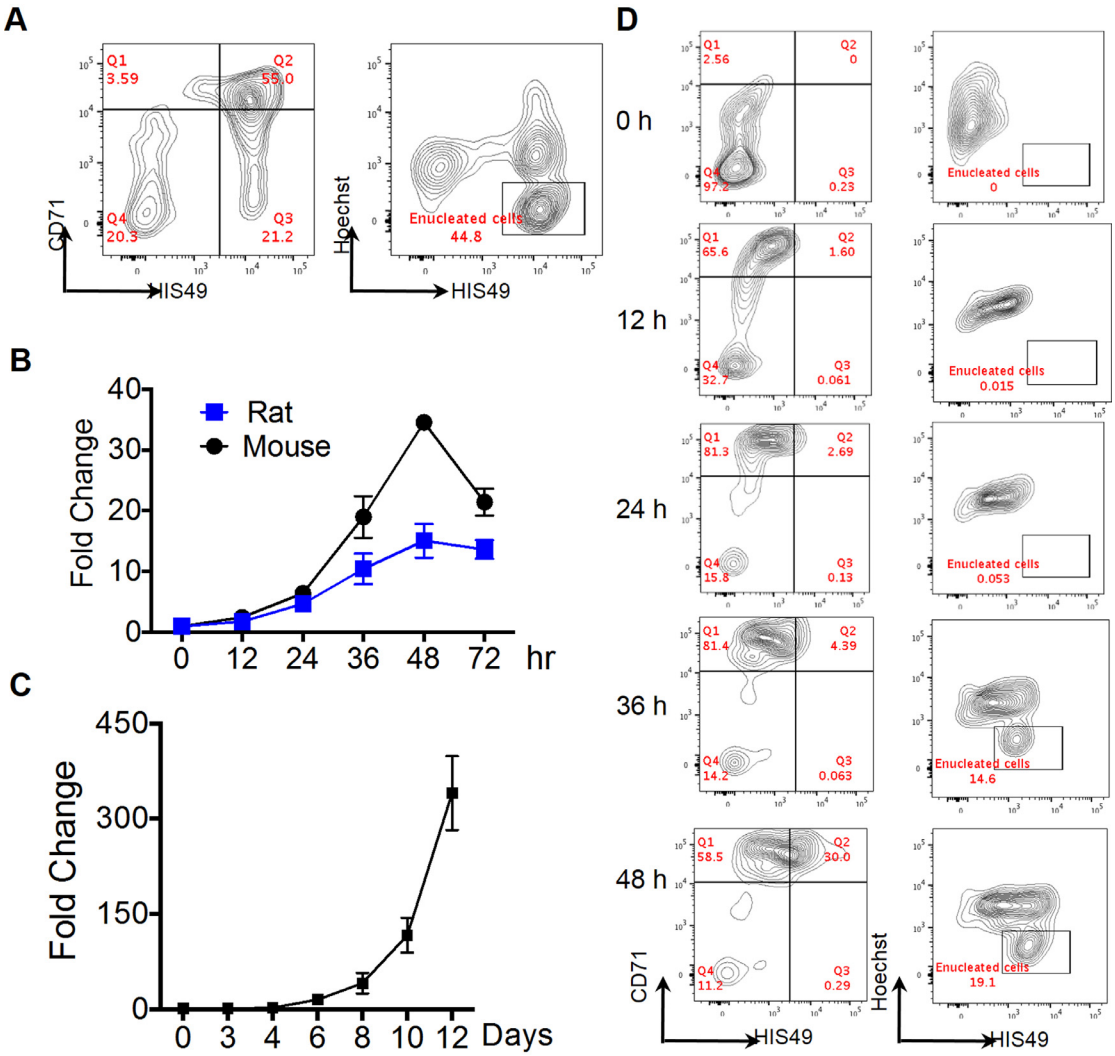

Supplemental Figure S1. In vitro culture of rat E13.5 fetal liver HIS49-negative cell. (A) Total survival fetal liver cells were gated based on CD71, His49 and Hoechst. (B) 6×10^4 purified Ter119-negative cells from mouse E13.5 fetal livers and His49-negative cells from rat E13.5 fetal livers were seeded on 6h and cell number were counted on indicated time point. There were triplicates in each time point. Fold change was analyzed as indicated. (C) After 4 days expansion, 6×10^4 human cord blood CD34+ cells were seeded on Day4 and fold changes were analyzed. For each time point, triplicate samples were analyzed. (D) Purified His49-negative rat fetal liver cells were cultured in EPO media and analyzed on indicated time points based on FSC, SSC, PI, CD71, His49 and Hoechst.

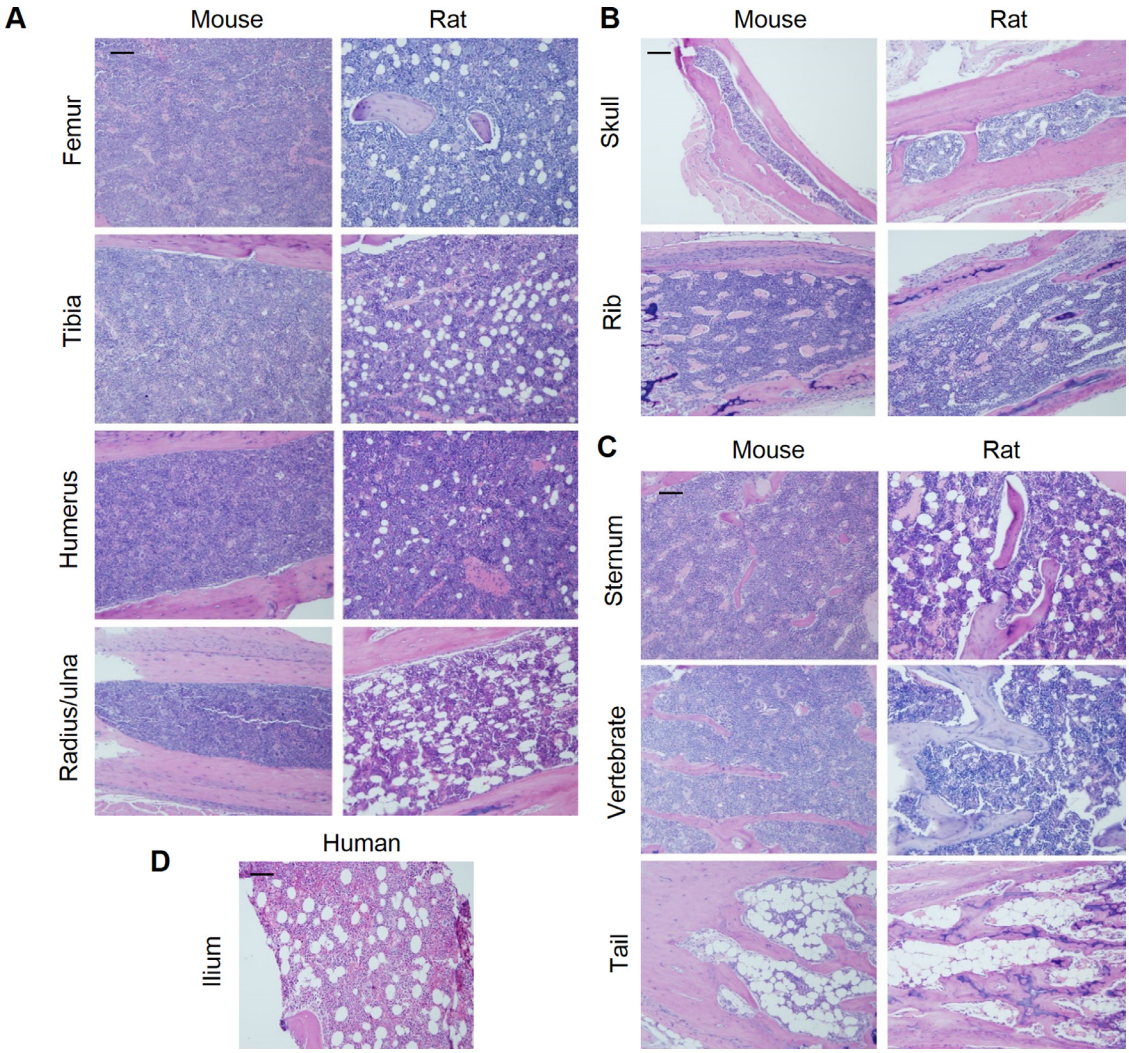

Supplemental Figure S2. Comparison of bone marrow cellularity in rats, mice, and humans. (A) Hematoxylin and eosin (H&E) staining of long bones including femur, tibia, humerus, radius/ulna in rats and mice. 6-8-week-old wild type C57BL/6 mice and 9-12-week-old wild type ACI rats were used. The pictures are representative of four animals in each species. (B) Same as A except flat bones including skull and rib were stained. (C) Same as A except irregular bones including sternum, vertebrate and tail bone were stained. (D) H&E staining of a human posterior ilium bone marrow core biopsy. Error bars: 100 μm.

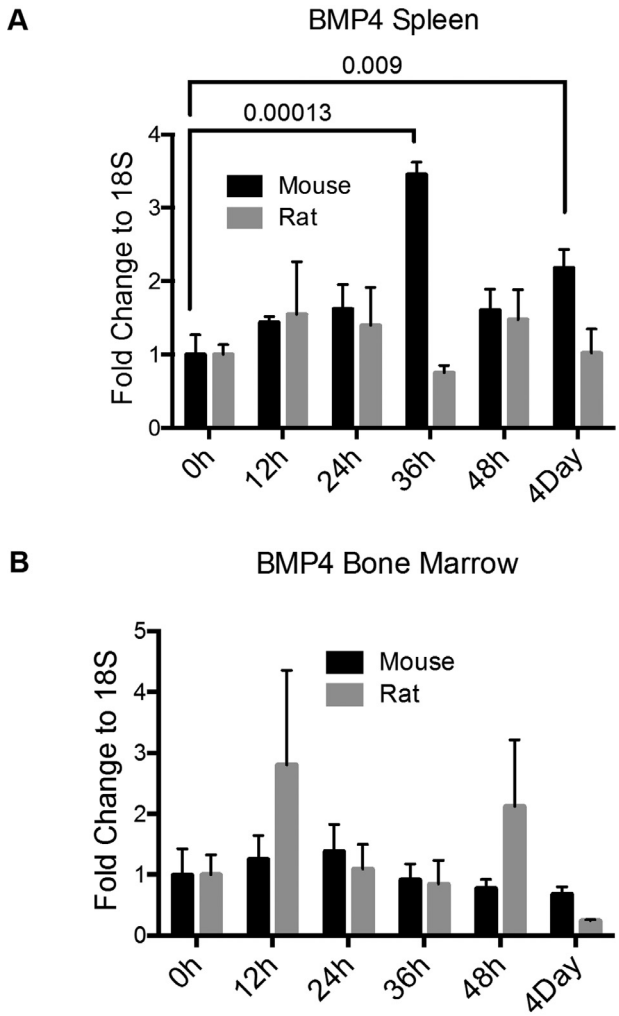

Supplemental Figure S3. BMP4 expression in rat and mouse spleen and bone marrow after one-time 100mg/kg PHZ treatment. Rats and mouse were injected with one-time 100mg/kg PHZ and sacrificed on indicated time point after treatment. Total RNA was extracted from total bone marrow or spleen cells and cDNA were reverse transcribed. (A-B) BMP4 expression level in rat and mouse bone marrow (A) and spleen (B) normalized with 18S rRNA.